

Implicit Multilinear Modeling of Air Conditioning Systems

Torben Warnecke¹ ^a and Gerwald Lichtenberg² ^b

¹*Deutsches Elektronen-Synchrotron DESY, Notkestr. 85, 22607 Hamburg, Germany*

²*Faculty of Life Sciences, Hamburg University of Applied Sciences, Ulmenliet 20, 21033 Hamburg, Germany*

Keywords: Multilinear Algebra, Differential-Algebraic Models, State-Space Models, Tensor Decomposition, HVAC, Air-Conditioning, Building Automation, Building Simulation.

Abstract: The publication explores the applicability of implicit multilinear model approaches in air conditioning systems. Implicit multilinear time-invariant models offer a structure that allows for the representation of most of the fundamental physical equations of HVAC systems. Since the implicit multilinear time-invariant model class is closed, it enables a component-based modeling approach to represent various types of HVAC systems with different combinations of components. Multilinear time-invariant models are usually represented by tensors. With HVAC-Systems having a large number of inputs and states, the models can be efficiently represented in a decomposed manner, resulting in a matrix representation. As an example, the model of a precision climatization hutch with a PI controller is derived and simulated.

1 INTRODUCTION


In this paper, an example model is provided to demonstrate the applicability of implicit multilinear time-invariant (iMTI) models for HVAC-Systems (Heating, Ventilation and Air Conditioning) working with humid air. The energy equations of HVAC-Systems mostly consist of linear combination of mass flows and thermodynamic states, such as temperatures or enthalpies (specific energy content of mass), e.g. in the first law of thermodynamics applied to fluids. Such equations typically exhibit a multilinear time-invariant structure, as shown in (Lichtenberg et al., 2022), (Pangalos et al., 2013) and (Pangalos et al., 2014). A multilinear time-invariant structure can be derived from the fundamental physical equations of thermodynamic states and the energy conservation principles of humid air systems. For the example of a precision climatization hutch, typical thermodynamic approaches, e.g. shown in (Yao and Yu, 2018), were used. Usually, these systems are approximated using linearized state-space models. However, this paper proposes a modeling method with fewer approximations, allowing for direct utilization of most of the fundamental physical equations.


2 MULTILINEAR MODELS

Recently, the implicit multilinear model framework has been introduced. Firstly in an explicit form in (Pangalos et al., 2013) and an implicit form in (Lichtenberg et al., 2022). The multilinear model method serves as a compromise between slow but accurate nonlinear and fast but linear models. Furthermore, linear and binary models can be fully represented using the multilinear structure. The multilinear functions enable the utilization of tensor algorithms and multilinear algebra, since the model structure and parameter-space can be represented by tensors. This facilitates the usage of tensor decomposition methods and enhances the efficient use of multilinear models in simulations or other applications, like control and automation.

2.1 Implicit Multilinear State-Space Modeling

Expanding the explicit multilinear time-invariant (eMTI) model format into the implicit multilinear time-invariant (iMTI) format allows the multiplication of state derivatives $\dot{\mathbf{x}} \in \mathbb{R}^n$ with states $\mathbf{x} \in \mathbb{R}^n$, inputs $\mathbf{u} \in \mathbb{R}^m$ and/or outputs $\mathbf{y} \in \mathbb{R}^r$. This enables the representation of broken rational functions within implicit multilinear models. More importantly, the iMTI model class is a closed model class, mean-

^a  <https://orcid.org/0009-0004-3037-8634>

^b  <https://orcid.org/0000-0001-6032-0733>

ing that any combination with different iMTI models results in the overall model still being an iMTI model. This includes representation of series, parallel and feedback connections, as demonstrated in (Lichtenberg et al., 2022). An iMTI model can be expressed as the inner tensor product of the model tensor

$$\mathbf{H} \in \mathbb{R}^{\overbrace{2 \times \dots \times 2}^{2n+m+r} \times e}, \text{ with } e \text{ being the application specific number of equations, and the monomial tensor } \mathbf{M}(\dot{\mathbf{x}}, \mathbf{x}, \mathbf{u}, \mathbf{y}) \in \mathbb{R}^{2^{2n+m+r}} \text{ by}$$

$$\mathbf{0} = \langle \mathbf{H} | \mathbf{M}(\dot{\mathbf{x}}, \mathbf{x}, \mathbf{u}, \mathbf{y}) \rangle. \quad (1)$$

The model tensor can be decomposed using the canonical polyadic (CP)-representation, shown in (Kruppa, 2017), and normalization methods proposed in (Jöres et al., 2022) into the norm-1 structure matrix $\mathbf{F} \in \mathbb{R}^{(2n+m+r) \times R}$ and the parameter matrix $\Phi \in \mathbb{R}^{e \times R}$, with R as the model rank given by the number of over-terms

$$\mathbf{H} = [\mathbf{F}, \Phi]. \quad (2)$$

In the decomposed form, the implicit system of equations can be constructed from the structure matrix \mathbf{F} and parameter matrix Φ without reconstructing the full tensor by inserting the matrices into the normalized factored polynomial

$$0 = \sum_{k=1}^R \Phi_{j,k} \prod_{i=1}^{2n+m+r} (1 - |\mathbf{F}_{i,k}| + \mathbf{F}_{i,k} \mathbf{v}_i) \quad (3)$$

with the variables $\mathbf{v} = \begin{pmatrix} \dot{\mathbf{x}} \\ \mathbf{x} \\ \mathbf{u} \\ \mathbf{y} \end{pmatrix}$ for all $j \in \{1, 2, \dots, e\}$.

3 PHYSICS OF AIR CONDITIONING SYSTEMS

To simplify the following equations and provide a rough overview of the given dynamics, an isobaric, respectively ambient pressure, system is considered, allowing the use of isobaric material properties. Because kinetic and potential energy differences in air streams of AC (air conditioning)-systems are small compared to enthalpy differences, those are neglected.

3.1 Enthalpy of Wet Air

The state of humid air can be adequately described by the independent states of temperature and humidity along with the isobaric material properties of dry air and water vapor. The specific enthalpy

$$h = c_d \vartheta + c_v \mu \vartheta + h_0 \mu \quad (4)$$

of wet air can be calculated with the temperature ϑ in $^{\circ}\text{C}$ and absolute humidity μ in $\text{kg}_{\text{water}}/\text{kg}_{\text{air}}$, where c_d represents the heat capacity of dry air, c_v the heat capacity of water vapor in the air and h_0 the evaporation enthalpy. Equation (4) is a multilinear function of temperature ϑ and humidity μ due to the second term of the equation, whereas the first and third terms are linear.

3.2 Energy and Humidity Transfer of a Wet Air Stream

To describe the energy absorbed by a mass flow q_m of air, the first law of thermodynamics for stationary flowing fluids can be applied. To calculate the change in enthalpy h_V and humidity μ_V in a given reference volume V , the following differential equations can be obtained

$$\rho V \dot{h}_V = q_m (h_{in} - h_{out}), \quad (5)$$

$$\rho V \dot{\mu}_V = q_m (\mu_{in} - \mu_{out}), \quad (6)$$

with ρ as density of the air, h_{in} as enthalpy of the entering and h_{out} as enthalpy of the exiting air.

The assumption is made that the air is well-mixed inside the reference volume and the air states are the same throughout the volume (principle of concentrated masses and lumped parameters). This assumption holds for small distances/volumes and high velocities. This means that the exiting air states are equal to the air states of the reference volume and the equations (5) and (6) can be rewritten as

$$\rho V \dot{h}_V = q_m (h_{in} - h_V), \quad (7)$$

$$\rho V \dot{\mu}_V = q_m (\mu_{in} - \mu_V). \quad (8)$$

For higher resolution or larger systems, multiple interconnected volumes (cells) can be used, as in CFD or FEM calculations.

To calculate the temperature ϑ_V of the reference volume, the additional algebraic equation

$$h_V = c_d \vartheta_V + c_v \mu_V + h_0 \vartheta_V \mu_V \quad (9)$$

is needed. Eq. (4) can be used for calculating the enthalpy h_{in} of the entering air stream from its temperature ϑ_{in} and humidity μ_{in} . Substituting (4) and (9) into (7) results in

$$\rho V \dot{h}_V = c_d q_m \vartheta_{in} + h_0 q_m \mu_{in} + c_v q_m \vartheta_{in} \mu_{in} - q_m h_V. \quad (10)$$

The differential equations (8) and (10) can be transformed into an implicit state-space model with the states $\mathbf{x} = (h_V \ \mu_V)^T$, inputs $\mathbf{u} = (q_m \ \vartheta_{in} \ \mu_{in})^T$ and output $y = \vartheta_V$ as follows

$$0 = \rho V \dot{x}_1 + u_1 x_1 - c_d u_1 u_2 - h_0 u_1 u_3 - c_v u_1 u_2 u_3 \quad (11)$$

$$0 = \rho V \dot{x}_2 + u_1 x_2 - u_1 u_3 \quad (12)$$

with the additional algebraic output equation

$$0 = x_1 - c_d y - c_v x_2 - h_0 y x_2. \quad (13)$$

The structure matrix \mathbf{F} of the iMTI model is

$$\mathbf{F} = \begin{pmatrix} 0 & 0 & 0 & 0 & 0 & 0 & 0 & 0 & 0 & 0 & 1 \\ 0 & 0 & 0 & 0 & 0 & 0 & 0 & 0 & 0 & 1 & 0 \\ 0 & 0 & 0 & 0 & 0 & 0 & 0 & 1 & 1 & 0 & 0 \\ 0 & 0 & 0 & 0 & 1 & 1 & 1 & 0 & 0 & 0 & 0 \\ 0 & 1 & 1 & 1 & 0 & 0 & 1 & 0 & 1 & 0 & 0 \\ 0 & 0 & 1 & 1 & 0 & 0 & 0 & 0 & 0 & 0 & 0 \\ 0 & 1 & 0 & 1 & 0 & 0 & 0 & 0 & 0 & 0 & 0 \\ 1 & 0 & 0 & 0 & 0 & 1 & 0 & 0 & 0 & 0 & 0 \end{pmatrix}. \quad (14)$$

The parameter matrix Φ is

$$\Phi^T = \begin{pmatrix} 0 & 0 & -c_d \\ -1 & -h_0 & 0 \\ 0 & -c_d & 0 \\ 0 & -c_v & 0 \\ 0 & 0 & -c_v \\ 0 & 0 & -h_0 \\ 1 & 0 & 0 \\ 0 & 0 & 1 \\ 0 & 1 & 0 \\ \rho V & 0 & 0 \\ 0 & \rho V & 0 \end{pmatrix}. \quad (15)$$

In the upcoming chapter, an iMTI model of an actual air conditioning system is developed to further investigate the practical applicability of this modeling approach.

4 EXAMPLE: CLIMATIZATION HUTCH

A precision climatization hutch for magnetic field measurements of magnets needed in particle accelerators will act as example for this study. The temperature in the climatization hutch needs to maintain at $21 \pm 0.1^\circ\text{C}$, to prevent warping of the magnets due to thermal expansion during the measurements. Therefore, the hutch is cooled by a recirculating air conditioning system, which is operated with a constant air flow and a high air exchange rate of approx. $20\ 1/\text{h}$ (which means that the air volume is completely replaced 20 times per hour). The system is shown in the Figure 1. The hutch itself is located inside an industrial hall. The air conditioning system consist of a duct system, a water-air heat exchanger with a mixing-valve operated with cooling water and a fan. The mixing valve is controlled by a PI-controller.

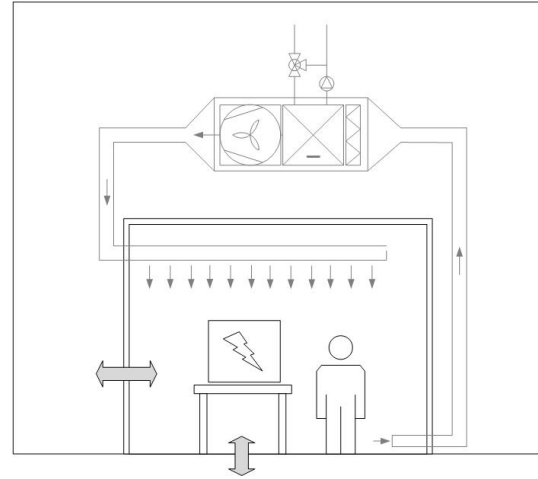


Figure 1: Climatization hutch with a recirculating air conditioning system (in grey).

4.1 Component-Based Modeling

The model consists of interconnected sub-models, including the room, air duct, dry water-air heat exchanger, mixing valve, walls, floor and PI controller. In the following sections each component will be described by thermodynamic equations.

4.1.1 Room

The thermodynamic behavior of the room can be described by the change \dot{E}_{room} of energy content of the room air. Often climatization zones are described by multiple cells, e.g. a 3-cell model with an air-supply, working and air-return cell, as shown in (Yao and Yu, 2018). To reduce the number of equations in this paper, a simpler one-cell model is represented. As before such a cell is considered well-mixed.

The example includes the energy exchange Q_{vent} due to ventilation, energy losses Q_{wall} towards the walls, energy losses Q_{floor} towards the floor and internal heat sources Q_{int} (like the magnet and the magnet power supplies). The heat losses from the fan motor are part of the internal heat sources, since it is a closed system.

The change of energy content of the room can be further described by the mass m_r times the change \dot{h}_r in enthalpy of the room air. The dynamic energy conservation law results in

$$m_r \dot{h}_r = Q_{vent} + Q_{wall} + Q_{floor} + Q_{int}. \quad (16)$$

The water content of the air is modeled by the dynamic mass conservation law, also called the continuity or transport equation. The change $\dot{\mu}_r$ in absolute humidity (mass of water per mass of air) can be calculated with the entering and exiting water vapor

mass flows. For simplification no internal gain rates of water vapor are modeled, only the exchanged vapor mass flow $q_{m,\mu,vent}$ due to ventilation is considered. The transport equation for the water vapor results in

$$m_r \dot{\mu}_r = q_{m,\mu,vent}. \quad (17)$$

Eq. (4) can be used to calculate the temperature ϑ_r implicitly from the enthalpy h_r and humidity μ_r of the room air

$$h_r = c_d \vartheta_r + c_v \mu_r \vartheta_r + h_0 \mu_r. \quad (18)$$

4.1.2 Air Duct

The air duct system supplies and removes air from the room. The energy rate Q_{vent} between the supplied air by the AC-unit and the room air is modeled using the first law of thermodynamics for stationary flowing fluids

$$Q_{vent} = q_{m,air} (c_d (\vartheta_{sup} - \vartheta_r) + c_v (\mu_{sup} \vartheta_{sup} - \mu_r \vartheta_r) + h_0 (\mu_{sup} - \mu_r)), \quad (19)$$

where $q_{m,air}$ is the mass flow of the exchanged air, ϑ_{sup} the temperature of the supplied air and μ_{sup} the absolute humidity of the supplied air.

The exchange rate $q_{m,\mu,vent}$ of water vapor due to ventilation is calculated by

$$q_{m,\mu,vent} = q_{m,air} (\mu_{sup} - \mu_r). \quad (20)$$

4.1.3 Dry Water-Air Heat Exchanger

A heat exchanger can be modeled by the energy content of the 2 liquids inside the exchanger and the energy storage of the exchange material itself. Overall the model has 3 energy storages. The concept of concentrated masses and lumped parameters is used and each storage is represented by one cell with one according mass. It is also possible to use multi-cell approaches for the different materials.

In the climatization hutch, the heat exchanger is used for cooling the air, but it is only operated with temperatures above 14°C, so the heat exchanger always operates in dry operation mode and no condensation appears.

The energy content of the air is modeled based on its average enthalpy $h_{a,av}$ and air mass m_a inside the heat exchanger. The airflow $q_{m,air}$ is similar in the whole system. The incoming air has the states of the room air (temperature ϑ_r and humidity μ_r) since it is directly extracted from the room. Duct heat losses are neglected. Since the heat exchanger is operated in a dry mode, the exiting humidity μ_{sup} equals the incoming humidity μ_r . The average enthalpy $h_{a,av}$ is calculated by the mean value of the entering and exiting

enthalpies h_r and h_{sup}

$$h_{a,av} = \frac{h_r + h_{sup}}{2}. \quad (21)$$

The enthalpy h_r can be calculated with (18). The supply temperature ϑ_{sup} can be calculated implicitly from the enthalpy h_{sup} and humidity μ_r by

$$h_{sup} = c_d \vartheta_{sup} + c_v \mu_r \vartheta_{sup} + h_0 \mu_r. \quad (22)$$

The change $m_a \dot{h}_{a,av}$ in energy content of the air includes heat dissipated from the airflow and heat transfer to the heat exchange material. The power balance for the air results in

$$m_a \dot{h}_{a,av} = q_{m,air} (h_r - h_{sup}) + k_a A_a \eta_{ex} (\vartheta_{ex,w} - \vartheta_{a,av}), \quad (23)$$

where k_a is the heat transfer coefficient of the air-side, A_a the heat transfer surface of the air-side, η_{ex} the heat exchange efficiency and $\vartheta_{ex,w}$ the surface temperature of the heat exchanger on the water-side.

The change in energy content of the heat exchange material is modeled by the change $\dot{\vartheta}_{ex,w}$ in temperature of the material on the water-side, the mass m_{ex} of the material and its heat capacity c_{ex} . The change in energy content includes the heat transfer between the water and heat exchange material, as well as the heat transfer between the air and heat exchange material

$$m_{ex} c_{ex} \dot{\vartheta}_{ex,w} = k_w A_w (\vartheta_{w,av} - \vartheta_{ex,w}) + k_a A_a \eta_{ex} (\vartheta_{a,av} - \vartheta_{ex,w}), \quad (24)$$

with the heat transfer coefficient k_w of the water-side, the heat transfer surface A_w of the water-side and the average temperature $\vartheta_{w,av}$ of the water inside the heat exchanger.

The energy content of the water is modeled by its mass m_w , its heat capacity c_w and its average temperature $\vartheta_{w,av}$, which is calculated by the mean of the inlet and outlet temperatures $\vartheta_{w,in}$ and $\vartheta_{w,out}$

$$\vartheta_{w,av} = \frac{\vartheta_{w,in} + \vartheta_{w,out}}{2}. \quad (25)$$

As for the air, the change in energy content of the water is similar to the heat absorbed by the water flow $q_{m,w}$ and the heat transfer from the heat exchange material

$$m_w c_w \dot{\vartheta}_{w,av} = c_w q_{m,w} (\vartheta_{w,in} - \vartheta_{w,out}) + k_w A_w (\vartheta_{ex,w} - \vartheta_{w,av}). \quad (26)$$

4.1.4 Mixing Valve

A valve inside the water circuit is used to control the output of the heat exchanger. For precision cooling usually a mixing circuit with a mixing valve is used.

The 3-way mixing valve is positioned at the inlet water stream, as it can be seen in Figure 1. With the mixing valve, the hotter outlet water can be mixed in the cold feed water, raising the inlet water temperature of the heat exchanger. With an additional pump the circuit is operated with a constant water flow $q_{m,w}$, so unnecessary oscillation can be avoided. To avoid damaging pressure spikes the actuator response time T_{valve} is high. The change \dot{x}_{valve} of the valve position is modeled as an integrator over the difference between the valve position x_{valve} and control signal $u_{controller}$ divided by the response time T_{valve}

$$\dot{x}_{valve} = \frac{u_{controller} - x_{valve}}{T_{valve}}. \quad (27)$$

The water inlet temperature $\vartheta_{w,in}$ of the heat exchanger is calculated using the mixing equation

$$\vartheta_{w,in} = x_{valve}\vartheta_{w,feed} + (1 - x_{valve})\vartheta_{w,out}, \quad (28)$$

with $\vartheta_{w,feed}$ as the feed temperature of the primary cooling water supply and $\vartheta_{w,out}$ as the water outlet temperature of the heat exchanger.

4.1.5 Wall and Floor

The walls and floor act as additional thermal energy storages and transfer heat with the room and environment. The change in energy content of these structures is modeled by the change $\dot{\vartheta}_{wall,i}$ of their temperatures times their masses $m_{wall,i}$ and heat capacity $c_{wall,i}$. The transferred heat is linearly depending on the temperature differences between the wall and adjacent zones. The power balance results in

$$m_{wall,i}c_{wall,i}\dot{\vartheta}_{wall,i} = k_{in,i}A_{wall,i}(\vartheta_r - \vartheta_{wall,i}) + k_{out,i}A_{wall,i}(\vartheta_{amb,i} - \vartheta_{wall,i}), \quad (29)$$

with the inner heat transfer coefficient $k_{in,i}$, the heat transfer surface $A_{wall,i}$, the outer heat transfer coefficient $k_{out,i}$ and the ambient temperature $\vartheta_{amb,i}$, which is the hall temperature in case of the walls and the ground temperature in case of the floor.

The heat $Q_{wall,i}$ transferred between the room and the wall/floor can be calculated by

$$Q_{wall,i} = k_{in,i}A_{wall,i}(\vartheta_{wall,i} - \vartheta_r). \quad (30)$$

In the example, the walls have been modeled as one wall, with their surfaces added to each other. The floor is modeled separately.

4.1.6 PI Controller

A PI controller is implemented in the model to maintain the desired room temperature. The controller signal $u_{controller}$ consists of a proportional and an integrating part. The proportional part is calculated via a

gain of K_P on the control error between the set temperature ϑ_{set} and the room temperature ϑ_r . The integrating part is calculated via a gain of K_I on the integrated control error. The equations of the PI controller result in

$$\dot{x}_I = \vartheta_{set} - \vartheta_r, \quad (31)$$

$$u_{controller} = K_P(\vartheta_{set} - \vartheta_r) + K_I x_I. \quad (32)$$

These equations describe the behavior of the components of the precision climatization hutch and can be used for simulation and analysis.

4.2 Overall Model

The overall model is built from the implicit state-space models of the single components. In the following those state-space models and the connection equations will be shown.

Since no condensation or humidity sources are modeled, the humidity is constant and could be treated as a parameter for the model. For demonstration purposes, it remains as a variable, it is expected that in further research those effects can be represented with iMTI models (see chapter 7).

The state-space model of the room has the states $[x_1 \ x_2]^T = [h_r \ \mu_r]^T$, inputs $[u_1 \ \dots \ u_5]^T = [Q_{vent} \ Q_{wall} \ Q_{floor} \ Q_{int} \ q_{m,\mu,vent}]^T$ and outputs $[y_1 \ y_2]^T = [\vartheta_r \ \mu_r]^T$. The equations of the state-space model are

$$\begin{aligned} 0 &= m_r \dot{x}_1 - u_1 - u_2 - u_3 - u_4, \\ 0 &= m_r \dot{x}_2 - u_5, \\ 0 &= c_d y_1 - x_1 + h_0 x_2 + c_v x_2 y_1, \\ 0 &= x_2 - y_2. \end{aligned} \quad (33)$$

The air duct state-space model has the inputs $[u_6 \ \dots \ u_{10}]^T = [\vartheta_r \ \mu_r \ q_{m,air} \ \vartheta_{sup} \ \mu_{sup}]^T$ and outputs $[y_3 \ y_4]^T = [Q_{vent} \ q_{m,\mu,vent}]^T$. The equations of the state-space model are

$$\begin{aligned} 0 &= c_d u_8 u_9 - c_d u_6 u_8 - y_3 - h_0 u_7 u_8 + h_0 u_8 u_{10} \\ &\quad - c_v u_6 u_7 u_8 + c_v u_8 u_9 u_{10}, \\ 0 &= u_8 u_{10} - u_7 u_8 - y_4. \end{aligned} \quad (34)$$

The duct model is connected to the room model via the connection equations

$$\begin{aligned} 0 &= u_1 - y_3, \\ 0 &= u_5 - y_4, \\ 0 &= u_6 - y_1, \\ 0 &= u_7 - y_2, \\ 0 &= u_{10} - y_2. \end{aligned} \quad (35)$$

The state-space model of the heat exchanger has the states $[x_3 \ x_4 \ x_5]^T = [h_{a,av} \ \vartheta_{ex,w} \ \vartheta_{w,av}]^T$, inputs $[u_{11} \ \dots \ u_{15}]^T = [q_{m,air} \ \vartheta_r \ \mu_r \ q_{m,w} \ \vartheta_{w,in}]^T$, outputs $[y_5 \ y_6]^T = [\vartheta_{sup} \ \vartheta_{w,out}]^T$ and auxiliary $z_1 = \vartheta_{a,av}$. The equations of the state-space model are

$$\begin{aligned} 0 &= 2c_d u_{11} u_{12} - 2u_{11} x_3 - m_a \dot{x}_3 + 2h_0 u_{11} u_{13} \\ &\quad + 2c_v u_{11} u_{12} u_{13} + A_a \eta_{ex} k_a x_4 - A_a \eta_{ex} k_a z_1, \\ 0 &= A_w k_w x_5 - x_4 (A_w k_w + A_a \eta_{ex} k_a) \\ &\quad - c_{ex} m_{ex} \dot{x}_4 + A_a \eta_{ex} k_a z_1, \\ 0 &= A_w k_w x_4 - A_w k_w x_5 - c_w m_w \dot{x}_5 \\ &\quad + 2c_w u_{14} u_{15} - 2c_w u_{14} x_5, \\ 0 &= h_0 u_{13} - x_3 + c_d z_1 + c_v u_{13} z_1, \\ 0 &= 2x_3 - c_d u_{12} - c_d y_5 - 2h_0 u_{13} - c_v u_{12} u_{13} - c_v u_{13} y_5, \\ 0 &= 2x_5 - u_{15} - y_6. \end{aligned} \quad (36)$$

The heat exchanger model is connected to the rest of the model with

$$\begin{aligned} 0 &= u_{12} - y_1, \\ 0 &= u_{13} - y_2, \\ 0 &= u_9 - y_5. \end{aligned} \quad (37)$$

The state-space model of the walls has the state $x_6 = \vartheta_{wall}$, the inputs $[u_{16} \ u_{17}]^T = [\vartheta_r \ \vartheta_{amb}]^T$ and output $y_7 = Q_{wall}$. The equations of the state-space model are

$$\begin{aligned} 0 &= A_{wall} k_{wall,in} u_{16} - A_{wall} (k_{wall,in} + k_{wall,out}) x_6 \\ &\quad + A_{wall} k_{wall,out} u_{17} - c_{wall} m_{wall} \dot{x}_6, \\ 0 &= A_{wall} k_{wall,in} x_6 - A_{wall} k_{wall,in} u_{16} - y_7. \end{aligned} \quad (38)$$

The state-space model of the floor has the state $x_7 = \vartheta_{floor}$, inputs $[u_{18} \ u_{19}]^T = [\vartheta_r \ \vartheta_{ground}]^T$ and output $y_8 = Q_{floor}$. The equations of the state-space model are

$$\begin{aligned} 0 &= A_{floor} k_{floor,in} u_{18} - A_{floor} (k_{floor,in} + k_{floor,out}) x_7 \\ &\quad + A_{floor} k_{floor,out} u_{19} - c_{floor} m_{floor} \dot{x}_7, \\ 0 &= A_{floor} k_{floor,in} x_7 - A_{floor} k_{floor,in} u_{18} - y_8. \end{aligned} \quad (39)$$

The wall and floor model is connected to the rest with

$$\begin{aligned} 0 &= u_{16} - y_1, \\ 0 &= u_{18} - y_1, \\ 0 &= u_2 - y_7, \\ 0 &= u_3 - y_8. \end{aligned} \quad (40)$$

The state-space model of the mixing valve has the state $x_8 = x_{valve}$, inputs $[u_{20} \ u_{21} \ u_{22}]^T =$

$[u_{controller} \ \vartheta_{w,feed} \ \vartheta_{w,out}]^T$ and output $y_9 = \vartheta_{w,in}$. The equations of the state-space model are

$$\begin{aligned} 0 &= u_{20} - x_8 - T_{valve} \dot{x}_8, \\ 0 &= u_{22} - y_9 + u_{21} x_8 - u_{22} x_8. \end{aligned} \quad (41)$$

The valve model is connected to the system model with

$$\begin{aligned} 0 &= u_{22} - y_6, \\ 0 &= u_{15} - y_9. \end{aligned} \quad (42)$$

The controller state-space model has the state $x_9 = x_I$, inputs $[u_{23} \ u_{24}]^T = [\vartheta_{set} \ \vartheta_r]^T$ and output $y_{10} = u_{controller}$. The equations of the state-space model are

$$\begin{aligned} 0 &= u_{23} - u_{24} - \dot{x}_9, \\ 0 &= K_P u_{23} - y_{10} - K_P u_{24} + K_I x_9. \end{aligned} \quad (43)$$

The controller model is connected to the system model with

$$\begin{aligned} 0 &= u_{24} - y_1, \\ 0 &= u_{20} - y_{10}. \end{aligned} \quad (44)$$

The resulting input and disturbance signals of the overall model are

$$\begin{aligned} \mathbf{u}_{open} &= [u_4 \ u_8 \ u_{11} \ u_{14} \ u_{17} \ u_{19} \ u_{21} \\ &\quad u_{23}]^T \\ &= [Q_{int} \ q_{m,air} \ q_{m,air} \ q_{m,w} \ \vartheta_{amb} \ \vartheta_{ground} \\ &\quad \vartheta_{w,feed} \ \vartheta_{set}]^T. \end{aligned} \quad (45)$$

The redundant inputs u_8 and u_{11} have been replaced by one input. The linear connection equations have been reduced by exchanging the variables y_i and u_j with one similar auxiliary variable z_k . In case of the variables ϑ_r and μ_r , they have been replaced by similar output variables.

The overall model has 9 states, 7 inputs, 2 outputs and 9 auxiliaries. The structure matrix \mathbf{F} can be stored as sparse boolean matrix and has the dimensions $\mathbb{R}^{36 \times 47}$ with 63 elements of one. The parameter matrix Φ can be stored as a sparse matrix with dimensions $\mathbb{R}^{20 \times 47}$ with 76 nonzero elements. The values for the model parameters are shown in the appendix.

This model construction process demonstrates that it is possible to directly represent a thermodynamic modeling approach of an HVAC system in an iMTI model. In the next chapter, simulation results are provided to showcase a practical application of the model.

5 SIMULATION

For simulation, the system of equations (3) is solved using the ode15i-solver from Matlab version 2022b.

Therefore initial values of the states and input trends are needed. The simulation represents the operation of 4 hours of an imaginary summer day in Germany.

5.1 Initial Conditions

For this example, the initial states are set as follows

$$\mathbf{x}_0 = [43488 \quad 0.008 \quad 43488 \quad 23 \quad 23 \quad 23 \quad 17 \quad 0 \quad 0]^T. \tag{46}$$

This refers to initial temperatures of 23°C for the room and walls, as well as the air and water inside the heat exchanger and the heat exchange material itself. The initial floor temperature is set to 17°C, since it is directly exposed to the ground. The initial room humidity is set to $8 \times 10^{-3} \text{ kg}_{\text{water}}/\text{kg}_{\text{air}}$. The mixing valve is completely closed and the initial controller signal is set to zero.

With the states and first input signals initial guesses for the state derivatives and outputs can be calculated with Eq. (3). The numerical solver `vpasolve` for symbolic equations is used.

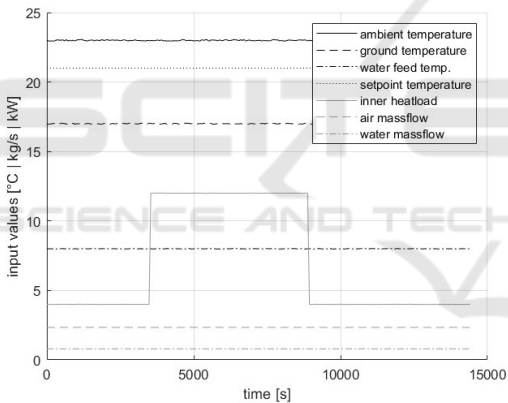


Figure 2: Input temperatures, mass flows and heatload.

5.2 Input Signals

The trends of the input signals are shown in Figure 2. The figure displays the temperature input signals ϑ_{amb} , ϑ_{ground} , $\vartheta_{w,feed}$ and ϑ_{set} , which are nearly held constant for better traceability of the model behavior, as well as the mass flows $q_{m,air}$ and $q_{m,w}$ of the air and water. Also the inner heatload Q_{int} of the climatization hutch is shown and represented as an rectangular function (in kW). This could represent when a magnet is powered and measurements of the magnetic field are conducted.

5.3 Results

Figure 3 presents the computed temperature trends, including the states: ϑ_{wall} , $\vartheta_{w,av}$, $\vartheta_{ex,w}$, and the output and auxiliary variables: ϑ_r , ϑ_{sup} , $\vartheta_{w,in}$, $\vartheta_{w,out}$. Figure 4 shows the controller signal $u_{controller}$ and the valve position x_{valve} . Based on experience with precision climatization, the results appear reasonable.

Notably, the responses to the up and down step of the inner heatload differ qualitatively from each other, particularly in the trend of the valve opening x_{valve} . This difference could be attributed to the non-linearities of the mixing valve’s sub-model, as other variables in multilinear terms are held constant.

Further research into other air conditioning systems, especially those using variable airflow and systems with humidification and dehumidification requirements, may reveal more of such behavior.

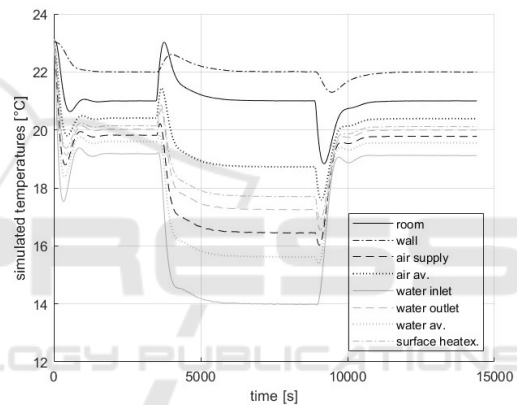


Figure 3: Simulated temperature signals.

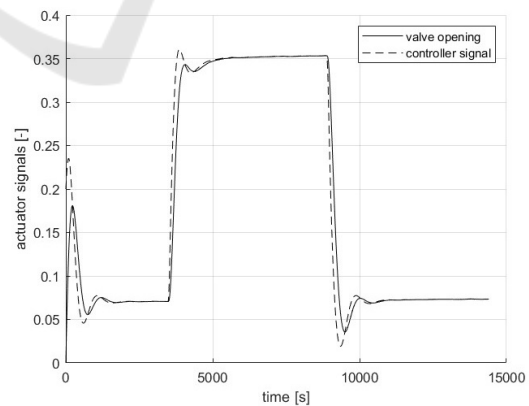


Figure 4: Simulated control signal and valve opening.

6 CONCLUSION

Implicit MTI models prove to be a suitable extension of the eMTI class for modeling complex HVAC-systems. These models can directly represent most physical laws and equations of HVAC systems, and offer the advantage of being a closed model class, simplifying component-based modeling and the use of standardized methods. They can be utilized in model-based applications, like nonlinear model predictive control to optimize competing goals, like energy consumption, comfort and technical compliances.

However, there are some limitations of the applicability of the iMTI class in HVAC systems. Non-integer exponents can't be represented by the iMTI formula, which may arise from empirical analysis for calculating convection heat transfer coefficients or dynamic flow resistances.

7 OUTLOOK

To account for the cooling of air below the saturation temperature ϑ_{sat} , which would involve the air cooler operating in a wet mode where condensation occurs and the air dehumidifies, additional binary signals are required. The resulting system would be a hybrid system with both binary and continuous signals, as well as additional inequality constraints. Future research will focus on investigating how binary variables can be implemented and simulated within the iMTI class.

Furthermore, the overall system can be potentially reduced further by redundant equations, variables and unnecessary states. This reduces storage capacity and computation time. Future research will explore automated methods for reduction of iMTI models.

ACKNOWLEDGMENTS

T.W. (DESY) acknowledges funding of the technical design phase of Petra IV granted by the Behörde für Wissenschaft, Forschung, Gleichstellung und Bezirke (BWFGB) of the Freie und Hansestadt Hamburg under the contract BWFG/F|97236, as well as by the Bundesministerium für Bildung und Forschung (BMBF) under the contract DES21TDR.

REFERENCES

Jöres, N., Kaufmann, C., Schnelle, L., Yáñez, C., Pangalos, G., and Lichtenberg, G. (2022). Reduced cp represen-

tation of multilinear models. *Proceedings of the 12th International Conference on Simulation and Modeling Methodologies, Technologies and Applications*.

Kruppa, K. (2017). Comparison of tensor decomposition methods for simulation of multilinear time-invariant systems with the mti toolbox * *this work was partly supported by the project observe of the federal ministry for economic affairs and energy germany (grant-no.: 03et1225b). *IFAC-PapersOnLine*, 50(1):5610–5615.

Lichtenberg, G., Pangalos, G., Cateriano Yáñez, C., Luxa, A., Jöres, N., Schnelle, L., and Kaufmann, C. (2022). Implicit multilinear modeling. *at - Automatisierungstechnik*, 70(1):13–30.

Pangalos, G., Eichler, A., and Lichtenberg, G. (2013). Tensor systems - multilinear modeling and applications. *Proceedings of the 3rd International Conference on Simulation and Modeling Methodologies, Technologies and Applications*.

Pangalos, G., Eichler, A., and Lichtenberg, G. (2014). Hybrid multilinear modeling and applications. *Advances in Intelligent Systems and Computing*, page 71–85.

Yao, Y. and Yu, Y. (2018). *Modeling and control in air-conditioning systems*. Springer Berlin.

APPENDIX

Parameters

A_a	A_{floor}	A_w
$20.8m^2$	$102.3m^2$	$5.22m^2$
A_{wall}	c_d	c_{ex}
$240.8m^2$	$1006J/kgK$	$477J/kgK$
c_{floor}	c_v	c_w
$900J/kgK$	$1860J/kgK$	$4200J/kgK$
c_{wall}	h_0	k_a
$650J/kgK$	$2.501 \times 10^6 J/kg$	$600 W/m^2K$
$k_{floor,in}$	$k_{floor,out}$	K_I
$2 W/m^2K$	$2 W/m^2K$	$-2 \times 10^{-4} 1/Ks$
K_p	k_w	$k_{wall,in}$
$-0.1 1/K$	$1000 W/m^2K$	$3 W/m^2K$
$k_{wall,out}$	m_a	m_{ex}
$3 W/m^2K$	$0.4341kg$	$42.5kg$
m_{floor}	m_r	m_w
$70000kg$	$418.8kg$	$27.75kg$
m_{wall}	T_{valve}	η_{ex}
$770.4kg$	$120s$	0.85